Intermolecular vibrations of large ammonia clusters from helium atom scattering

Titus A. Beu,[a] Christof Steinbach, and Udo Buck[b]
Max-Planck-Institut für Strömungsforschung, Bunsenstraße 10, D-37073 Göttingen, Germany

(Received 20 February 2002; accepted 29 May 2002)

The excitation of the low-energy intermolecular modes of ammonia clusters by helium atom scattering has been calculated using classical trajectories. The energy transfer is investigated as a function of scattering angle (from 10° to 90°), collision energy (94.8 and 50.5 meV), cluster size ($n=18$, 100, 1000), and cluster temperature ($T_c=1$ K, 30–50 K, and 105 K). It is observed that predominantly the mode at 7 meV and to a lesser extent also the one at 12 meV are excited. These are surface modes that mainly originate from the angular motion of three adjacent N atoms. The excitation is nearly independent of the cluster size and the probability for multiphonon excitation steadily increases with increasing deflection angle. This trend is even strengthened by increasing the collision energy. The role of the cluster temperature is to broaden the energy transfer distribution with increasing values. The calculations are compared with previous and new measurements presented here of the double-differential cross sections $(d\sigma/d\omega)_{\Delta E}$ of ammonia clusters of average size $\langle n\rangle=92$ at two collision energies and $\langle n\rangle=1040$ at one energy. While the general trends in the angular and energy dependence could be well reproduced, the correct cluster temperature was crucial in getting good agreement at the lower collision energy for $n=100$. At the higher collision energy, the large energy transfer is not reproduced, probably a shortcoming of the potential models to account correctly for the anharmonicity of the strong multiquantum excitations. © *2002 American Institute of Physics.* [DOI: 10.1063/1.1494778]

I. INTRODUCTION

The structure and dynamics of hydrogen bonded clusters play a key role in a variety of research fields ranging from solvent-solute interactions to atmospheric chemistry. Most of the information on these systems comes from the spectroscopy of the intramolecular modes of the molecules in the infrared spectral range.[1] In exceptional cases also intermolecular modes have been measured using vibration-rotational-tunneling spectroscopy.[2] We have recently developed in our laboratory a tool that allows us to measure the low-energy intermolecular vibrations which evolve towards the phonon spectra of the condensed phases.[3] By observing the inelastic energy exchange of helium atoms scattered from argon clusters in the size range of $\langle n\rangle=22-4500$, we were able to demonstrate that mainly surface modes and their overtones were excited.[4,5] The transferred energy decreases from about 6 meV to 2 meV with increasing cluster size at collision energies of 25 meV and converges to the surface Rayleigh mode of solid argon.[4] Similar experiments have been carried out for water clusters of the average sizes $\langle n\rangle=11$, 22, 80, and 194 (Refs. 6–8) and for ammonia clusters of $\langle n\rangle=18$, 745, and 1024 (Ref. 9). In contrast to the results for argon, the energy transfer increases slightly with increasing cluster size. In the case of water, accompanying calculations demonstrated that at 5.5 meV mainly the O-O-O bending motion of three-coordinated surface molecules was excited.[6] For ammonia clusters which exhibit larger energy transfers in the range from 6 to 60 meV no calculations were available. We note that the collision energy for the molecular clusters was with 57/72 meV for water and 91/100 meV for ammonia clusters, much larger than the 25 meV used in the argon cluster experiment.

In the present contribution we essentially carry out such calculations for the vibrational excitation of ammonia clusters in collisions with helium atoms. We also added a measurement for the average size $\langle n\rangle=92$ at a smaller collision energy of 50 meV, in contrast to the 91–100 meV that was used in the previous experiments.[9] The cluster size distribution was measured with the help of a newly established method; namely, by doping the cluster by one sodium atom.[10] This gives, especially for smaller cluster sizes, more reliable, nearly fragmentation-free results. This new method led us to a new assignment of the lowest size distribution of the published results in Ref. 9.

We will carry out calculations for the sizes $n=18$, 100, and 1000. In this way we cover the largest amorphous cluster of our recent structure calculations of small ammonia clusters[11] and two crystalline clusters for which measurements are available. These will include static properties such as the structure and the spectra of the intermolecular vibrations. Here we use classical trajectories, applying simulated annealing and the calculation of the Fourier transform of the velocity autocorrelation function. For the calculation of the excitation probabilities of the vibrational spectrum in collisions with helium atoms, we also use classical trajectories. In the detailed analysis of the scattering of argon clusters from

[a]Permanent address: University "Babeş-Bolyai," Faculty of Physics, Department of Theoretical Physics, 3400 Cluj-Napoca, Romania.
[b]Electronic mail: ubuck@gwdg.de

helium atoms we found that single quantum excitations are better treated quantum mechanically, while multiphonon excitations were reproduced quite well using classical trajectories.[5] The reason for the partial failure of the classical calculations has to do with the boxing problem that allocates intensity below the smallest allowed transition frequency, so that the distinction between elastic and inelastic events becomes rather vague. On the other hand is the quantum mechanical treatment of a huge number of vibrational modes, as they occur for sizes up to $n=1000$, by no means straightforward. The methods which we used in our previous calculations, the sudden approximation for $He+Ar_{55}$ (Ref. 5) and first-order time-dependent perturbation theory for $He+(H_2O)_{90}$ (Ref. 6) already contain a couple of approximations and the main sizes to be treated here are even larger. In addition, the collision energy in the ammonia cluster experiments is within 50–100 meV higher than that of the previous experiments with argon clusters where 25 meV had been used. Therefore we prefer in the present calculations, because of the large size and high collision energy, the classical treatment and accept possible small deviations at low excitation frequencies.

II. EXPERIMENT

The experimental results for the average sizes $\langle n\rangle=18$, 745, and 1040 at collision energies between 90.8 and 99.8 eV were published in a previous publication.[9] Here we add a new measurement at a lower energy of 50.5 eV.[12] In the course of this work we discovered that the determination of the lowest size in one of the measurements of Ref. 9 was not correct. We repeated the size measurement using a new, more reliable technique. We will briefly report these new corrected results here.

The experiments have been carried out in a crossed molecular beam machine which is described in detail elsewhere.[13] The helium atom and the $(NH_3)_n$ cluster beams are generated in separate, differentially pumped source chambers and intersect each other at 90° in the scattering chamber. The angular dependence of the scattered intensity is measured by rotating the source assembly around the scattering center, while the detector unit, consisting of an electron impact ionizer combined with a quadrupole mass filter and a secondary-electron multiplier, is kept fixed. It is operated in a doubly differentially pumped chamber under ultrahigh-vacuum conditions. The velocity of the scattered helium atoms is measured by time-of-flight analysis using a pseudorandom chopper, located between the scattering center and the detector, with a flight path of 450 mm.

The helium atom beam is produced by expansion of the gas under the stagnation pressure of 16 bars through a small orifice with a diameter of 30 μm at a source temperature of $T_0=77$ K. Under these conditions the relative width of the velocity distribution is $\Delta v/v=0.017$ which leads to the energy resolution of about 3.4 meV at a collision energy of 50.5 meV. Typical parameters of the helium beam are given in Table I. For completeness we also list the data of the helium beam leading to a higher collision energy where a room temperature helium beam is used.

TABLE I. He and $(NH_3)_n$ beam data.

	He	$(NH_3)_n$	He	$(NH_3)_n$
Nozzle pressure p_o (bar)	16.0	3.0	16.0	3.0
Nozzle diameter d_o (μm)	30	100	30	100
Temperature T_o (K)	77	307	300	300
Peak velocity v_{max} (m/s)	1025	1178	1799	1159
Speed ratio S	87	16	96	17
Collisional energy E (meV)	50.5		94.8	
Mean cluster size $\langle n\rangle$	-	92	-	92

The $(NH_3)_n$ cluster beam is generated by expansion of ammonia of 3 bars through a plain orifice with a diameter 100 μm at a temperature $T_0=300$ K. The corresponding data and the resulting collision energies are also presented in Table I. The beam contains a distribution of cluster sizes, which we have analyzed using a reflectron time-of-flight mass spectrometer in which the $(NH_3)_n$ clusters are ionized by single photon ionization after they have been doped by one sodium atom.[10] With a fixed photon energy of 3.13 eV we are at the threshold of the trimer. The larger clusters have ionization potentials down to 2.0 eV at about $n=100$.[14] Thus, at most, about seven molecules might be evaporated. Figure 1 shows the actual distribution for the experimental conditions of Table I. The measured sizes follow log-normal distributions with the average cluster sizes of $\langle n\rangle=92$ and the halfwidth extends to about the same value. This is much larger than the previously published value of $\langle n\rangle=18$ for similar source conditions. Apparently the previous measurement was hampered by fragmentation caused by multiphoton processes.[15] The results for the larger clusters proved to be correct. We have added the new results for the higher collision energy also in Table I.

III. TIME-OF-FLIGHT AND ENERGY LOSS SPECTRA

The information on the vibrational excitation is obtained from time-of-flight (TOF) spectra taken at different laboratory deflection angles Θ. The new result for $\langle n\rangle=92$ at the low collision energy $E=50.5$ meV is shown in Fig. 2. The spectrum is dominated by the elastic contribution with $\Delta E=0$. At lower velocities and longer times, the inelastic contributions follow. They extend in the present measurement up

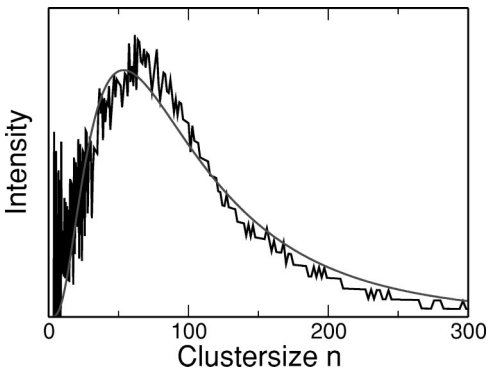

FIG. 1. Measured mass spectra of the ammonia cluster $(NH_3)_n$ beam the source conditions of which are given in Table I. The solid line is a fit of a log-normal distribution with the average size $\langle n\rangle=92$.

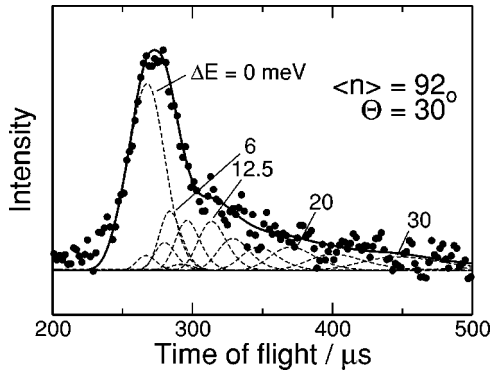

FIG. 2. Measured time-of-flight spectra for the average cluster size $\langle n \rangle = 92$ at the laboratory deflection angle of $\Theta = 30°$. The solid line is a fit to the spectra based on contributions of different energy transfers ΔE. Some important ones are presented by dashed lines and denoted by ΔE in meV. $\Delta E = 0$ meV represents the elastic cluster and monomer scattering which are counted together. The width is calculated from the resolution of the apparatus.

to $\Delta E = 30$ meV where they are cut off because of kinematical reasons. To relate these results to energy loss spectra in the center-of-mass (c.m.) system, we have to apply the standard procedure for this conversion which takes into account the resolution of the apparatus.[16] The number of particles per time unit (t) is given by the expression

$$\frac{dN(\Theta,t)}{dt} = \sum_{\Delta E} n_1 n_2 \Delta\Omega \Delta V \left(\frac{d\sigma}{d\omega}\right)_{\Delta E}(\theta) \times G_{\Delta E}(\Theta,t;v_1,v_2,\theta); \quad (1)$$

n_1 and n_2 are the densities of the helium and cluster beams, respectively, the scattering volume is represented by ΔV, and the solid angle of the detector is denoted by $\Delta\Omega$. The function $G_{\Delta E}(\Theta,t;v_1,v_2,\theta)$ contains the Jacobi factor for the c.m. (θ) to the laboratory (Θ) transformation with the velocities v_1 and v_2. It is calculated by a Monte Carlo procedure using the measured widths of the velocity distributions, the angular divergences of the two intersecting beams, the finite size of the scattering volume and the detector, and the resolution of the TOF analyzer.[16] The calculated width at half maximum of the distribution functions is 3.4 meV for the energy loss and 1.0° for the angular resolution. We note that the energy resolution of our experiment, though still quite good for a molecular beam experiment, is only moderate compared with the low frequencies of the cluster spectrum. The angular resolution is high, but since trajectories are used in the calculation of the angular dependence, theoretically, a resolution of only $\pm 2.5°$ is obtained.

This procedure can now be used in a twofold way. One possibility is to determine by a least-squares fit procedure to the measured dN/dt the cross sections in the c.m. system. The overall result of the fit is represented by the solid lines in the TOF spectra. Some of the single contributions given by dashed lines and marked by the corresponding energy transfers ΔE in meV are also shown. The selection of these contributions is somewhat arbitrary and also not complete. It only serves for a better understanding of the TOF spectra. Unfortunately the contributions of the elastically scattered helium atoms from the monomers cannot be distinguished from those which are elastically scattered from the clusters. Therefore these contributions are counted together and drawn as a single contribution in the time-of-flight spectra marked by $\Delta E = 0$ in meV.

It is noted here that in the angular range covered in the cluster experiments, the inelastic excitation of the ammonia monomers[17] and the ammonia dimers[18] in collisions with helium are quite small so that it is not necessary to take them into account in the data evaluation. The largest contribution at 30° gives an energy transfer of 10.7 meV with a cross section of about 1 Å^2/sr, which is usually less than 10% of the cluster cross section.

The typical results of such a transformation into c.m. coordinates will be presented in Sec. VI. We note that this procedure is not always exact, since the different inelastic contributions might belong, although taken at the same laboratory angle, to different c.m. angles. Therefore a direct comparison with calculations has to be considered with care. For such a comparison (and this is the second application of the averaging procedure), a better and unambiguous way is to transform the calculated cross section into the laboratory time-of-flight spectra using the same formalism. We will also present such results in Sec. VI.

IV. COMPUTATIONAL DETAILS

A. Classical trajectories calculations

The computer simulations reported in this work are based on classical molecular dynamics (MD). Three types of calculations have been carried out, in accordance with the investigated properties of the ammonia clusters: (a) geometrical structures, (b) vibrational spectra, and (c) scattering cross sections for the scattering of He atoms. Throughout the work, the ammonia monomer was considered nonrigid and its interactions with itself and with the He atom have been modeled by the site-site interaction potentials described in Sec. IV B. The MD integrator found to work most reliably, especially in the scattering simulations, where typically small energy differences are involved, was found to be the Verlet integrator,[19] known to rigorously ensure energy conservation. The geometrical equilibrium structures of the clusters have been determined by the method of simulated annealing.[20]

In order to characterize the overall vibration of the clusters, the classical *velocity autocorrelation function* was employed, since its Fourier-transform spectrum can be straightforwardly identified with the vibrational spectrum of the clusters. For the investigation of the low-frequency modes, specialized autocorrelation functions for the N-N bond stretching and the N-N-N angle bending motions have been defined, as well. In all spectrum simulations we have integrated the equations of motion over 8 ps with a time step of 2×10^{-4} ps, corresponding to a resolution in the frequency of 2.1 cm^{-1} (0.26 meV).

For each cluster size, the autocorrelation functions have been averaged prior to the Fourier transform over as many as 100 identical clusters, each cluster of the ensemble being assigned an initial excitation energy in accordance with the

Boltzmann distribution for the considered temperature. With a view to simplifying the interpretation of the simulated scattering data in conjunction with the vibrational spectra, the temperature assigned to each cluster size in the spectrum simulations was the one estimated in the scattering experiments, 30 K for $(NH_3)_{18}$ and 50 K for the larger clusters. Typically, the averaged correlations drop during the first 0.5 ps of the simulation below 10% of their initial values.

The trajectories for the He-$(NH_3)_n$ scattering have been described in the center-of-mass frame of the total system. In order to achieve reliable statistics, for the scattering involving the $(NH_3)_{18}$ and $(NH_3)_{100}$ clusters 100 000 trajectories are considered. Due to the extreme computational effort, in the case of $(NH_3)_{1000}$ only 12 800 trajectories are calculated.

For each trajectory, the initial conditions are specified by the impact parameter b, by the relative velocity $v_{\rm rel}$, and by the three Euler angles (α,β,γ), by which the cluster is rotated with respect to its own center of mass, in order to account for the arbitrary relative directions of incidence of the He atom. The impact parameter b was chosen randomly from a uniform distribution in the interval $[0,R_0+10\ \text{Å}]$, where R_0 is the radius defining the geometrical extent of the particular cluster. For the relative velocity $v_{\rm rel}$, values between 1560 and 2200 m/s (resulting from the experimental conditions) have been considered. The Euler angles have been chosen by uniformly sampling the whole space of angular orientations.

In addition to the mentioned initial conditions, the scattering simulations have proved very sensitive to the initial vibrational energy of the cluster $E_{\rm kin}$. For a specified cluster temperature T_c, the initial vibrational energy was randomly chosen for each trajectory in accordance with the corresponding Boltzmann distribution.

The quantities calculated for each single trajectory are the scattering angle θ, the interaction time τ, and the net energy transfer from He to the ammonia cluster, ΔE. The scattering angle θ is defined by the directions of the initial and final momentum vectors of the He atom. The interaction time τ is considered to be the interval between the moments when the absolute value of the potential energy of the He atom in the asymptotic region exceeds and, respectively, drops below 0.1 meV. The energy loss ΔE is defined as the difference between the relative kinetic energy (of the reduced He-atom–ammonia-cluster system) at the beginning and at the end of the trajectory.

Qualitatively, the crucial impact of the cluster temperature T_c on the computed energy loss spectra is evidenced by quite narrow profiles at low temperatures, with maxima located at low energy transfers, as opposed to the broad profiles for higher temperatures.

B. Interaction potential

The interaction potential that we have employed to describe the NH_3 clusters is the site-site potential used by Diraison *et al.*[21] in their MD simulations of liquid ammonia and denoted by F-KI. It actually consists of the simple site-site intermolecular potential of Impey and Klein[22] (KI) plus a harmonic valence force intramolecular potential, as applied to XY_3 molecules.[23]

TABLE II. Parameters for the He-NH_3 site-site potential.

	A_i (meV)	B_i (Å^{-1})	C_i (meV Å^6)
N	428355	3.233	12896.6
H	158065	4.356	889.7

Within the KI intermolecular potential, the NH_3 monomer is considered rigid and its geometry is defined by the nitrogen-hydrogen distance $r_{\rm NH}=1.0124$ Å and the angle between the N-H bonds and the C_3 axis of the molecule (pointing away from the H atoms), $\varphi_{\rm HNC_3}=112.13°$. This potential features electrostatic and Lennard-Jones interactions. The electrostatic interaction is modeled by four interaction sites on each molecule: three sites with partial charge $q_{\rm H}=0.462e$ located at the H atoms and a site with a charge $-3q_{\rm H}$ located on the C_3 axis, 0.156 Å from the N atom towards the H atoms. Lennard-Jones interactions are modeled only between the N atoms by a 12-6 potential with parameters $\sigma=3.4$ Å and $\epsilon/k_{\rm B}=140$ K.

The intramolecular potential for the NH_3 monomer implies three NH stretching and three HNH bending coordinates:

$$V_{\rm NH_3}=\frac{k_s}{2}(\delta r^2_{\rm NH_1}+\delta r^2_{\rm NH_2}+\delta r^2_{\rm NH_3})+\frac{k_b}{2}(\delta\varphi^2_{\rm H_1NH_2}+\delta\varphi^2_{\rm H_2NH_3}+\delta\varphi^2_{\rm H_3NH_1}),$$

where $\delta r_{\rm NH_i}$ represents the instantaneous deviation from the equilibrium NH_i bond length, while $\delta\varphi_{\rm H_iNH_j}$ is the instantaneous deviation from the equilibrium H_iNH_j bend angle. The values of the parameters are $k_s=39.633$ eV/Å^2 and $k_b=3.454$ eV.

In order to describe realistically and, at the same time, conveniently the interaction between the He atom and the NH_3 monomers within the scattering simulations, we have constructed a site-site model potential. The model parameters have been determined by fitting the elaborate *ab initio* potential energy surface developed by Meyer *et al.*[17] to model the rotationally inelastic He-NH_3 scattering. The functional form of our site-site potential features standard (exp-6) interaction terms between the He atom and all the atoms of the NH_3 monomer:

$$V_{\rm He\text{-}NH_3}=\sum_i\ [A_i\exp(-B_ir_i)+C_i/r_i^6],$$

where $i=\rm N,H_1,H_2,H_3$ and r_i represents the distance between atom i of the ammonia monomer and the He atom. All relevant data for this potential model are summarized in Table II. The quality of the fit achieved by our site-site potential can be judged from Fig. 3, where it is compared with the original potential of Meyer *et al.* for four combinations of polar angles (ϑ,ϕ). We mention that the coordinate system has fixed axes in the ammonia molecule, its origin is located in the center of mass, and the z axis coincides with the symmetry axis of the NH_3 molecule (the three H atoms are located in a perpendicular plane). The polar angles ϑ and ϕ

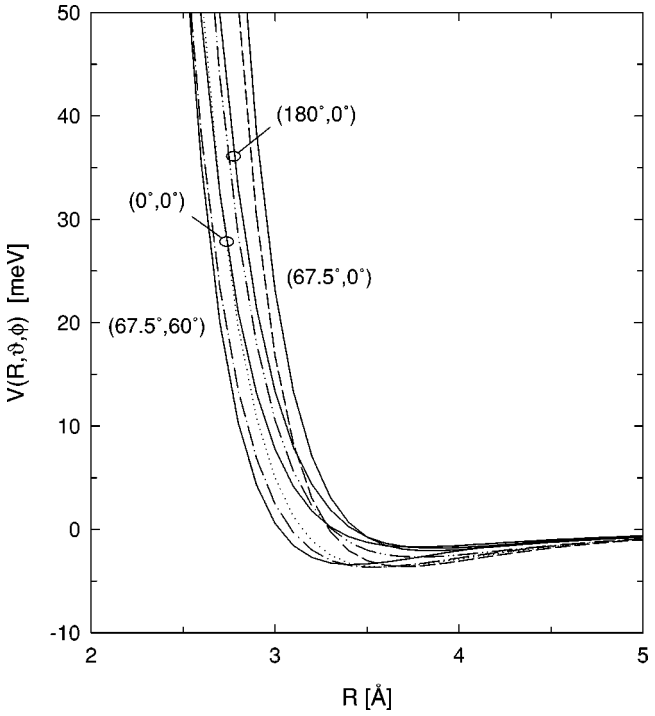

FIG. 3. Comparison between the He-NH_3 site-site potential and the *ab initio* potential of Meyer *et al.* (solid lines) for selected orientations.

measure the angles from the z axis and x-z plane, respectively. R is the distance from the He atom to the origin.

V. RESULTS

A. Structures

As found relevant for the comparison with the experimental data, we have considered three ammonia cluster sizes 18, 100, and 1000. In all cases, the structure calculation started from a well-defined initial configuration, which was initially heated to 100 K, in order to relax the surface molecules, and then cooled for approximately 10 ps with a time step of 10^{-4} ps, by removing 1% of the kinetic energy at each time step.

In the structure calculation of the $(NH_3)_{18}$ cluster, the initial configuration of the annealing process was just the equilibrium configuration we have reported in Ref. 11 and which was obtained by considering rigid ammonia monomers and the same NH_3-NH_3 intermolecular potential as in the present study. The final equilibrium configuration yielded by the present simulation considering nonrigid monomers is more compact, as expected, showing a binding energy of -427.8 kJ/mol (as compared to the initial value of -392.5 kJ/mol).

For $(NH_3)_{100}$ and $(NH_3)_{1000}$ the initial configurations have been chosen to be spheres cut from crystalline ammonia. Electron diffraction studies with large clusters of several thousands of molecules clearly demonstrate that these clusters adopt the cubic structure of the bulk, space group $P2_13$.[24] This solid-state structure of ammonia was extracted from the neutron diffraction study of Reed and Harris,[25] while the rest of the details of the annealing procedure have been the ones described above. The binding energies obtained for the two cluster sizes have been -2729.2 kJ/mol and -31113.1 kJ/mol, respectively. As can be seen from Figs. 4 and 5, the two clusters predominantly preserve a crystalline inner structure after the annealing process, still showing the characteristic hexagonal symmetry of the ammonia crystal along the [111] direction. The coordination number is 6 with three hydrogen and three covalent bonds.

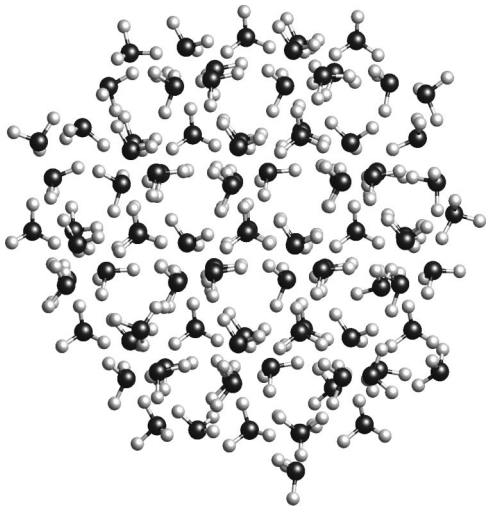

FIG. 4. Calculated structure of the $(NH_3)_{100}$ cluster.

We note that in this complicated multiminima problem we are not sure of having found the correct global minimum. This is, however, not very critical, since also in the experiment the system might have been trapped in one of the many closely lying, local minima. This is particularly valid at the relatively high, finite temperatures of the clusters in the present experiments.

B. Frequency spectra

The low-energy spectrum of the intermolecular modes of the ammonia clusters was determined by calculating the Fourier transform of the velocity autocorrelation function based on MD trajectories. The results for $n=18$ and 100 at finite

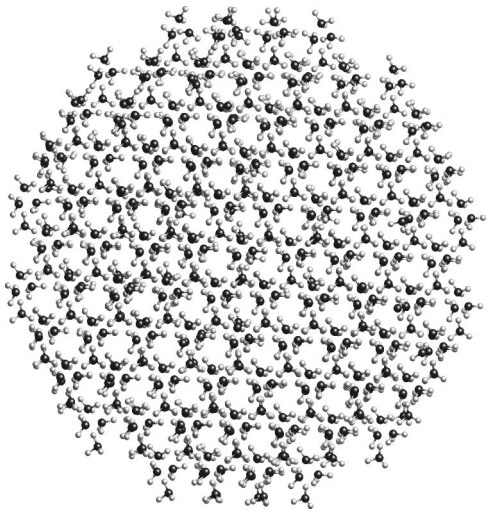

FIG. 5. Calculated structure of the $(NH_3)_{1000}$ cluster.

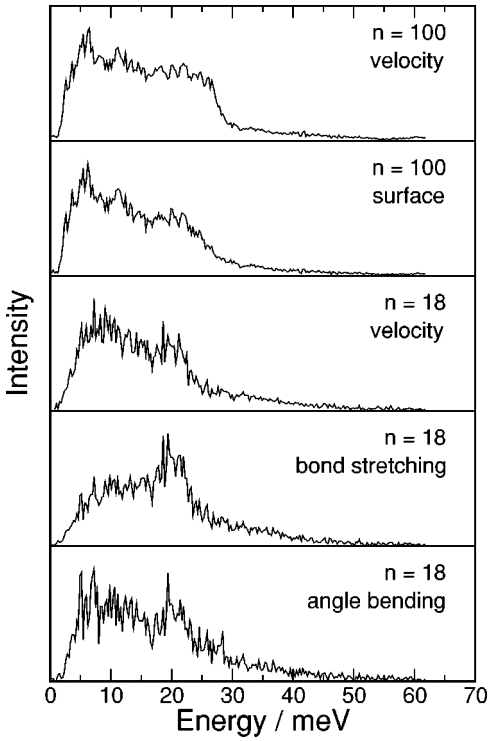

FIG. 6. Fourier transform of the autocorrelation function of different motions and different ammonia clusters. From top to bottom: $n=100$, velocity; $n=100$, velocity, surface modes only; $n=18$, velocity; NN bond stretch; NNN angular bending. The cluster temperature is 50 K and 30 K, respectively.

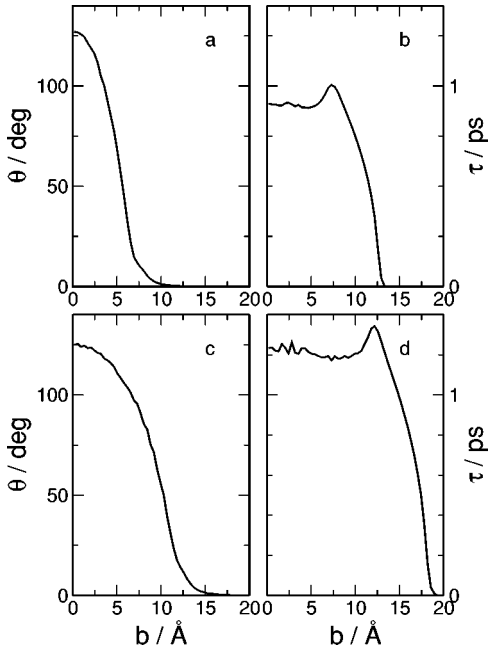

FIG. 7. The average deflection function θ and the average interaction time τ between the helium atom and the cluster as function of the impact parameter. (a),(b) $n=18$, cluster temperature $T_c=30$ K; (c),(d) $n=100$, $T_c=50$ K. The collision energy is in both cases $E=94.8$ meV.

temperatures are shown in Fig. 6. The spectrum of $n=18$ exhibits two broad peaks, one in the range between 6 and 8 meV with a shoulder at 12 meV and one around 20 meV. The spectrum of $n=100$ looks similar with the exception that the fall off at high energies is shifted from 22 to 28 meV. If we restrict the vibrational modes to those at the surface, the spectrum of $n=100$ is nearly identical to that of $n=18$, which mainly consists of surface modes with peaks at 7 meV, 12 meV, and 20 meV. Thus the additional modes around 25 meV are attributed to volume modes.

These results can be compared with those obtained for solid ammonia. Here four spectral lines are observed at 13.3 meV (A), 16.0 meV (E), 17.5 meV (F), and 22.8 meV (F) by Raman and infrared spectroscopy with their respective symmetry in parentheses.[26] Two broad distributions centered around 12 meV and 18 meV result from inelastic neutron scattering.[27] The theoretical interpretation attributes these vibrations to the translational motion of the heavy nitrogen atoms.[28,29] Since all these excitations are volume modes, there is only a weak correlation between the cluster and the bulk modes. The low-energy mode at 7 meV is a specific surface mode of the clusters, while the one at 25 meV is definitely a volume mode. Those modes between these two limits are surface modes in the cluster and volume modes in the crystal.

For water clusters, simple models were invoked to suggest that the lowest-frequency modes correspond to O···O···O bending skeletal vibrations between adjacent hydrogen bonds, while the next group of states corresponds to the O-O stretch of the hydrogen bonds. To verify these suggestions for ammonia clusters, we have calculated the power spectra of the angular motion of three adjacent N atoms and the N-N stretch motion. The results are also shown in Fig. 6. The bond stretching is largest in the third peak and goes down in the direction of the two smaller peaks. In contrast, the angular bending motion is more or less equally distributed over the three peaks. We conclude that the first two peaks are dominated by the bending motion, while the third one at the highest energy is more influenced by the stretching motion. But in contrast to the results for water, the two kinds of motions cannot be completely disentangled.

C. Vibrational excitation

In order to determine which part of the calculated frequency distribution has been excited in the collisions with helium atoms, we have calculated classical trajectories and analyzed them in terms of the deflection angle θ, the interaction time τ, and the energy loss ΔE. In total about 100 000 trajectories have been calculated for each of the figures that follow to present the doubly differential cross section $(d\sigma/d\omega)_{\Delta E}$. In case of deviations from this number, we will mention that.

Figure 7 shows the results for the average scattering angle θ and the interaction time τ as function of the impact parameter b for the two systems $He+(NH_3)_{100}$ (c),(d) and $He+(NH_3)_{18}$ (a),(b). The cluster temperature is $T_c=50$ and 30 K, respectively, and the collision energy $E=94.8$ meV in both cases. In both deflection functions, the scattering angle at $b=0$ is much smaller than 180°. This is a well-known effect, which was observed previously,[5,30] and originates from the roughness of the cluster surface that scatters the helium atoms in a distribution of directions. The interaction

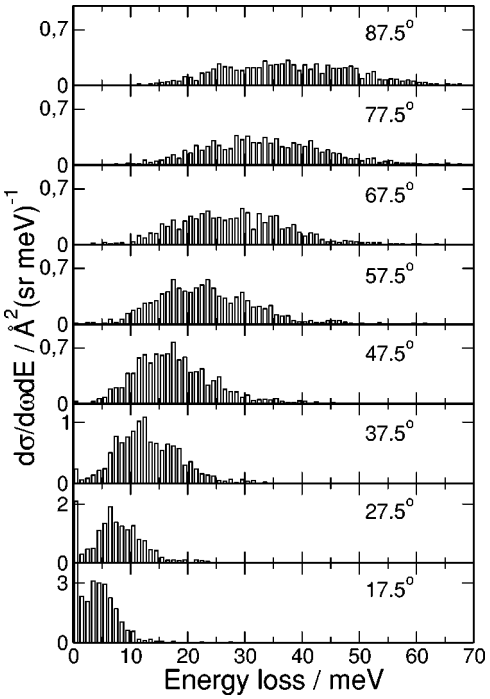

FIG. 8. Calculated cross sections for $He+(NH_3)_{100}$ as a function of the energy transfer ΔE for different scattering angles θ in the c.m. system. The collision energy is 94.8 meV and the cluster temperature $T_c=1$ K.

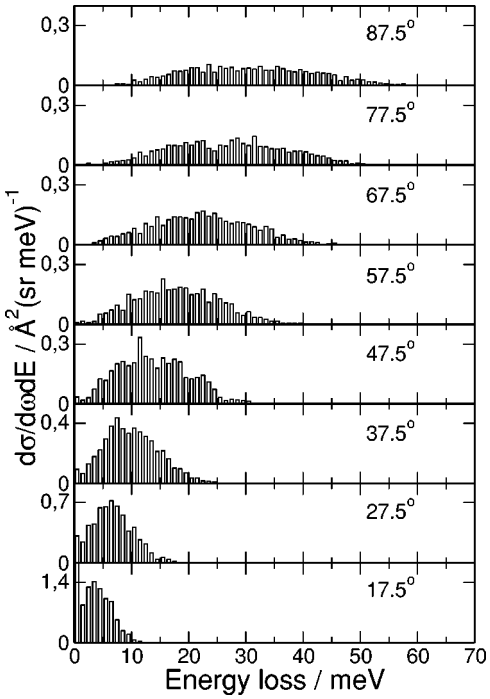

FIG. 9. Calculated cross sections for $He+(NH_3)_{18}$ as a function of the energy transfer ΔE for different scattering angles θ in the c.m. system. The collision energy is 94.8 meV and the cluster temperature $T_c=1$ K.

time is almost constant for small impact parameters, rises to a maximum, and then falls off to zero when the helium atom does not hit the cluster directly anymore. The maximum occurs when the helium atom enters the attractive part of the potential. As expected, the value at which the falloff occurs is larger for the larger cluster.

The energy transfer from the helium atom to the cluster $n=100$ is displayed in Fig. 8 for a series of c.m. scattering angles from $\theta=17.5°$ to 87.5°. The events were sampled in angular intervals of $\pm 2.5°$ and the width of the energy boxes is 1.0 meV. The collision energy is 94.8 meV and the cluster temperature $T_c=1$ K. As expected, the vibrational energy transfer is small in the forward direction, since the coupling is very weak for these large impact parameters. With increasing scattering angle, the amount of elastic scattering at $\Delta E=0$ decreases, while the energy transfer rapidly increases. This is certainly an effect of the stronger coupling for the more direct collisions. At deflection angles between 20° and 30° the peak of the distribution occurs at 6 meV. With increasing scattering angle it moves to 15 meV at 47.5° and 35 meV at 87.5°. The latter distribution extends to energy transfers of about 60 meV.

If we compare the calculated energy transfer with the frequency distribution of the Fourier transform of the velocity autocorrelation function of Fig. 6 for this cluster size, it is immediately clear that the scattering at large deflection angles is dominated by multiphonon excitations. According to the detailed results obtained for the scattering of helium atoms from argon clusters,[4,5] the full spectrum for the excitation of a single phonon is already reached at about 20°. This means that only the first part of the available frequency spectrum is excited in helium atom scattering. The frequency range is governed by the angular motion of adjacent N atoms. This result is quite similar to that observed for water clusters in this size range where only the bending motion of the O atoms is excited.[6] With increasing deflection angle, the energy transfer is completely dominated by multiphonon excitations up to the point where no intensity is left at the position of the single-phonon excitation.

The results for two other cluster sizes $n=18$ and $n=1000$, taken under otherwise similar conditions, are shown in Fig. 9 and 10. The general picture of the results for $n=18$ is very similar to the one obtained for $n=100$. For $n=1000$, where only the small angular range from 0° to 30° was covered by cutting the impact parameter for $b\leqslant 20$ Å and where, in addition, only 12 800 trajectories have been calculated, the peaks are less pronounced and broader. But the behavior is similar taking into account the less reliable statistics.

Finally, the results of two other important changes are presented in Figs. 11 and 12 for $n=100$. These are the influence of the cluster temperature and the collision energy on the energy transfer. We estimated initially the temperature of our ammonia clusters $T_c=50$ K from the value obtained recently from the deexcitation of water clusters in collisions with helium.[6] We found $T_c=69-101$ K in the size range $\langle n\rangle=80-194$. Since the binding energy is somewhat smaller for ammonia, the lower value $T_c=50$ K was specified. There is, however, another value available obtained by electron diffraction studies of much larger ammonia clusters in the size range of some thousands of molecules ($d=8$ nm). The authors calculated that the cluster temperature is $T_c=115$ K for our experimental time scales.[24] Based on these results, we estimate a value of $T_c=105$ K for smaller clusters $\langle n\rangle$

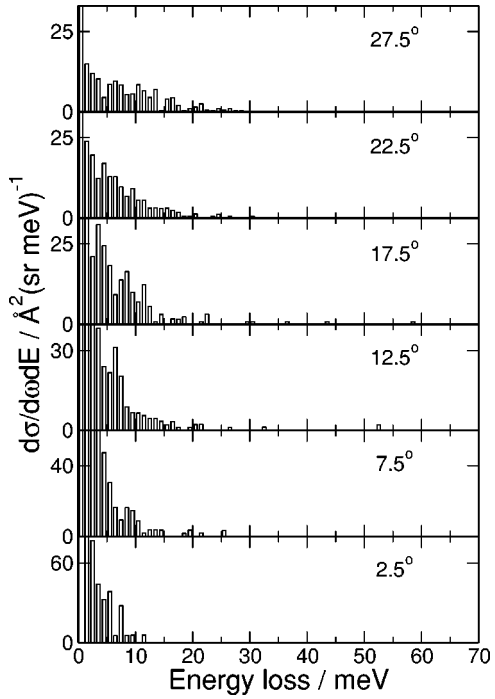

FIG. 10. Calculated cross sections for $He+(NH_3)_{1000}$ as a function of the energy transfer ΔE for different scattering angles θ in the c.m. system. The collision energy is 83.4 meV and the cluster temperature $T_c=1$ K.

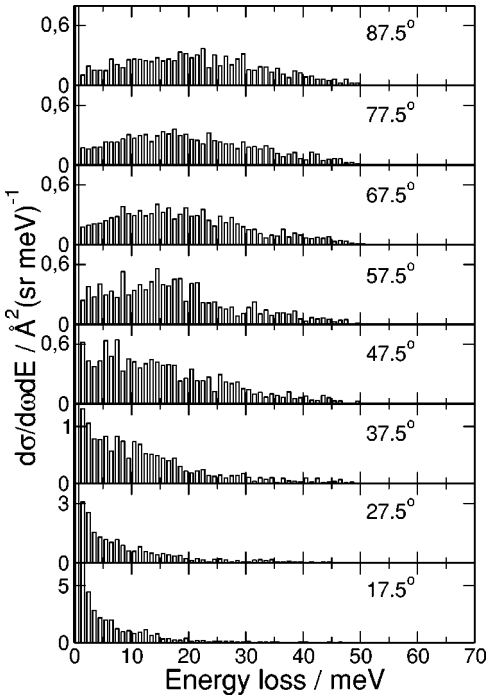

FIG. 12. Calculated cross sections for $He+(NH_3)_{100}$ as a function of the energy transfer ΔE for different scattering angles θ in the c.m. system. The collision energy is 50.5 meV and the cluster temperature $T_c=105$ K.

$=100$. The calculation for the cluster temperatures $T_c=50$ K and 105 K leads qualitatively to the same angular distributions with similar positions of the maximum but much broader widths caused by the increased internal motion. The big change takes place between $T_c=1$ K and 50 K, while the results for $T_c=105$ K are only marginally broader than those for 50 K. Thus we plotted in Fig. 11 only the results for $T_c=105$ K.

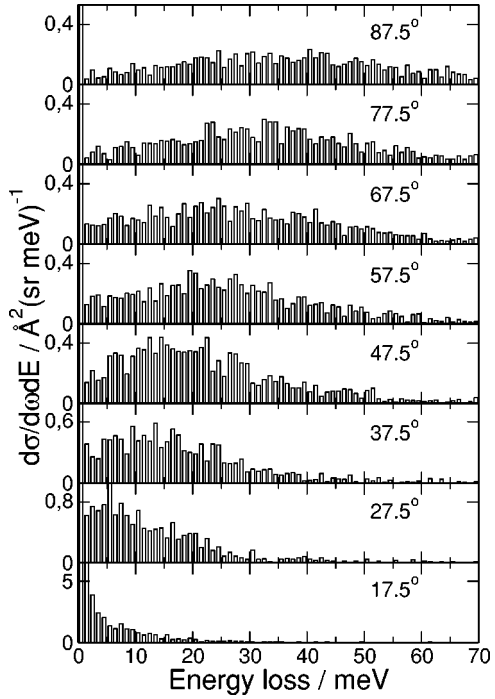

FIG. 11. Calculated cross sections for $He+(NH_3)_{100}$ as a function of the energy transfer ΔE for different scattering angles θ in the c.m. system. The collision energy is 94.8 meV and the cluster temperature $T_c=105$ K.

The effect of the lower collision energy, when going from 94.8 to 50.5 meV, is displayed in Fig. 12. It leads to a drastic shift of the maxima of the distribution by 10–20 meV towards smaller values. Apparently the quantity $\Delta E/E$ is constant, a result that is also found in many energy transfer processes in atom-molecule scattering.[31]

The calculations, in particular those for $n=100$, have been carried out by averaging over many trajectories. Aside from the usual initial-state distributions, the additional sampling over the different vibrational kinetic energies that correspond to the finite cluster temperatures leads to a number of different initial configurations, although we start from the same geometric configuration.

Finally, we have to discuss the reliability of the classical calculation. There are mainly two drawbacks in these calculations. The first has to do with the boxing problem. The energy of the first vibrational state is clearly separated from the elastic value. In the classical calculation, all energies are available and, therefore, especially the region between the elastic peak and the appearance of the first inelastic transition is not correctly reproduced. Second, classical mechanics does not account for the zero-point energy. If it is artificially added to account for the correct energy balance, it can flow into other modes. Detailed calculations for the system $He+Ar_n$ revealed that the first effect plays indeed a role in this type of helium-cluster collisions and leads, for small angles and single-phonon excitations, to an incorrect description. In fact, the rise of the cross section due to the first inelastic transitions occurs at too small energy losses. In con-

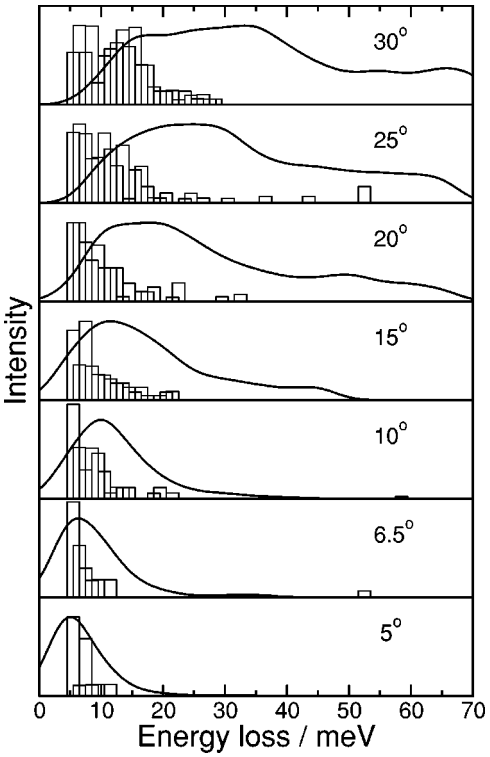

FIG. 13. Energy loss spectra for the averaged cluster size $\langle n \rangle = 1040$ at laboratory deflection angles in the range from $\Theta = 5°$ to $\Theta = 30°$ but transformed into the center-of-mass system (solid lines). The histograms are the calculated cross section for $n = 1000$ for the c.m. variables which correspond to the indicated laboratory scattering angles.

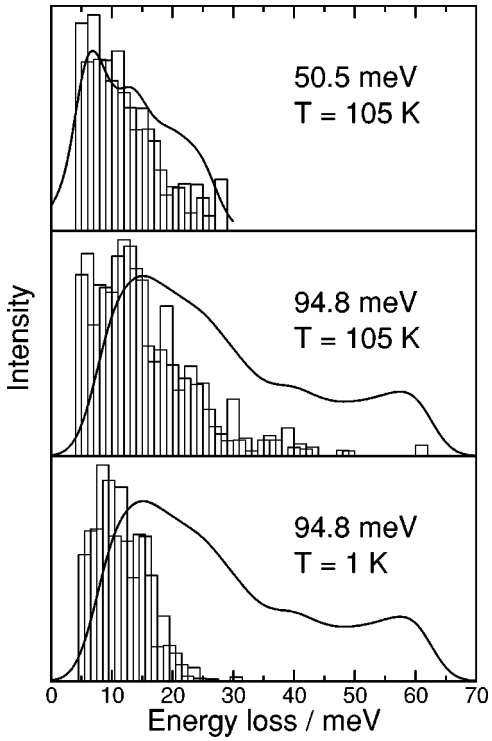

FIG. 14. Energy loss spectra for the averaged cluster size $\langle n \rangle = 92$ at laboratory deflection angle $\Theta = 30°$ but transformed into the center-of-mass system. The histograms are the corresponding calculated cross sections for $n = 100$. The different collision energies and cluster temperatures are indicated.

trast, multiphonon excitations are equally well reproduced by classical mechanics and quantum calculations.[5]

Since the present experiments are dominated by multiphonon excitations, this part is certainly reproduced well by the classical calculation. In addition, the collision energy is in the present experiments up to a factor of 4 higher than that used in the calculation of $He+Ar_n$. This effect should be again in favor of a reliable description of the scattering process by classical mechanics. The only problem left is the incorrect reproduction of the energy transfer at small scattering angles close to the elastic scattering peak. In order to observe this effect the energy resolution must be quite high, as was the case for $He+Ar_n$, where the transition of 1.6 meV could be clearly resolved at a collision energy of 25 meV. In the present experiments, with the same type of transitions but collision energies of 50 and 90 meV, the resolution is worse and thus the effect is less pronounced.

VI. COMPARISON WITH EXPERIMENT

The most detailed experimental results have been obtained for the average cluster size $\langle n \rangle = 1040$. The energy loss spectra at seven laboratory deflection angles and collision energy of $E = 99.8$ meV are presented in Fig. 13 as solid lines. Here the cross sections which are proportional to the fitted amplitudes are also averaged over the experimental resolution of the apparatus. They can directly be compared with the calculations for $He+(NH_3)_{1000}$ at an energy of $E = 83.4$ meV and temperature $T_c = 1$ K. The results of Fig. 10 are sampled in bins of 3.3 meV according to the experimental resolution and according to the c.m. contributions to the measured laboratory angles. The outcomes are also shown in Fig. 13. For the smaller deflection angles 5°, 6.5°, and 10°, where the coupling is weak, there is good agreement between experiment and calculations. At 15° and 20°, the regime of excitation of single vibrational quanta, we find too high intensity for small inelastic transitions, the expected boxing problem of the classical calculation. In addition, the intensity for large energy transfers is too small. For the largest angles measured, 25° and 30°, where multiphonon excitation starts to occur, the agreement at small transfers up to 15 meV is better but the intensity at large transfers is also missing here. The main reason for the discrepancy is not so much the different energies but certainly the unphysical cluster temperature $T_c = 1$ K of the calculations. Since a new calculation for $n = 1000$ was too time consuming, we will compare the smaller cluster size directly with the calculations at $T_c = 105$ K.

We compare the measurements that always contain a distribution of cluster sizes with calculations based on a single size. This is justified by the fact that the angular distribution of the intermolecular vibrational energy transfer only marginally depends on the cluster size under otherwise equal conditions. This is nicely demonstrated in the comparison of Fig. 8 and Fig. 9 for $n = 100$ and $n = 18$, which exhibits nearly the same pattern.

The resulting energy loss spectra for the average cluster size $\langle n \rangle = 92$ of the measurement of Fig. 2 and the corrected

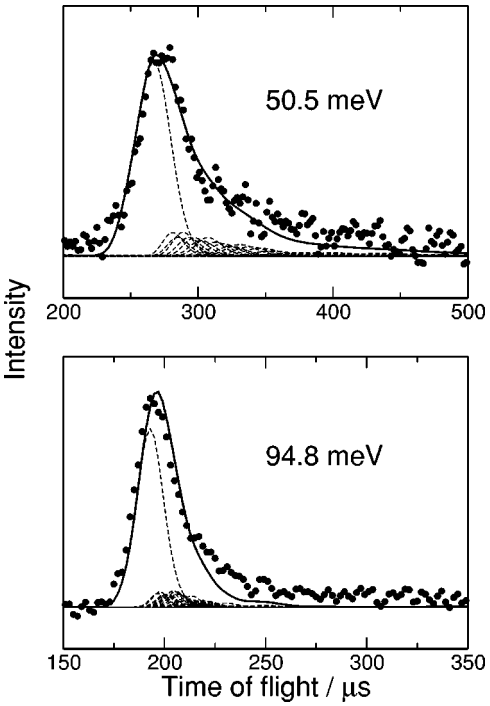

FIG. 15. Time-of-flight spectra for the average cluster size $\langle n \rangle = 92$ at laboratory deflection angle $\Theta = 30°$. The solid (sum) and dashed (single contributions) lines are calculated cross sections for $n = 100$ (see histograms in Fig. 14) transformed into the laboratory system. Upper panel: $E = 50.5$ meV. Lower panel: $E = 94.8$ meV. The cluster temperature is $T_c = 105$ K.

one of Ref. 9 at the higher energy are shown in Fig. 14 as solid lines. The results exhibit marked differences in the energy transfer for the two energies. At the lower energy, the distribution peaks at 7 meV with a shoulder at 12 meV. At the higher energy, the peak position is at 12 meV and the distribution exhibits a long tail up to transfers of 60 meV.

We already know from the comparison of the calculations for $n = 100$ at different temperatures, displayed in Fig. 8 and Fig. 11, that the distributions for the higher temperature are much broader. Therefore we compare in Fig. 14 first the results of these calculations at $T_c = 1$ K and 105 K with the measured data at the laboratory angle of 30° and collision energy of $E = 94.8$ meV. The agreement is much better for the higher temperature, but still not satisfying. In particular, at large energy transfers, the calculated intensity is too weak. The same calculation for the lower collision energy is in much better agreement with the data. The peak at 7 meV is well reproduced, and only at larger energy transfers is one of the shoulders not well reproduced.

To check the role of the laboratory-c.m. transformation with respect to these discrepancies and to see how far away the calculated results are from the measured data, we have carried out the same comparison in the laboratory system. The results are displayed in Fig. 15. For the lower collision energy, the agreement is again quite satisfactory. For the larger collision energy, the agreement is good in the range of the elastic peak, which mainly consists of the monomer contribution and the smaller inelastic parts. The discrepancies start to appear at larger energy transfers, but they are much less pronounced than in the c.m. system.

VII. DISCUSSION AND CONCLUSIONS

We have investigated the vibrational energy transfer of the low-energy intermolecular modes of ammonia clusters in collisions with helium atoms using classical trajectories. The vibrational spectrum that was obtained from the Fourier transform of the velocity autocorrelation function of different trajectories consisted of peaks at 7, 12, and 20 meV. From this spectrum only the range between 7 and 12 meV is excited in helium collisions. These are predominantly the surface modes of the angular motions of adjacent N atoms belonging to three different molecules in the cluster. At small deflection angles from 5° to 10° the coupling is too weak to excite this part of the spectrum. The range from 15° to 25° is dominated by single vibrational transitions. For angles larger than 25°, multiquantum excitations occur and at even larger angles the maximum intensity is already shifted away from the position of the single excitations. The comparison with the experimental data for $n = 1000$ reveals that the agreement is good for the small-angle region. In the single-excitation range the calculations predict too small energy transfers, due to boxing problems, below the first inelastic quantum channel. For the multiphonon range these problems disappear, but the intensity for large energy transfers is much too small. This is the general behavior that is already known from detailed investigation of the excitation of argon clusters. Classical trajectories are a good approximation for small angles that are dominated by weak coupling and large angles that are controlled by multiphonon processes. The discrepancy with the measurement is mainly traced back to the low cluster temperature of 1 K in the calculation. Indeed, if the temperature is increased to 105 K, the comparison of data and calculations improves for $n = 100$, especially for the lower collision energy. But there are still discrepancies at large energy transfers for the higher collision energy that are definitely caused by multiphonon processes. This is an unexpected result, since classical trajectories should work well in this regime. At these high energies, we are in a regime of highly excited intermolecular modes where the anharmonicity of the interaction potential plays an important role. Apparently, this part of the potential is not good enough for reproducing the measurements. We repeated the calculations with rigid molecules by using a formalism based on quaternions. In this case, we even observed narrower distributions. Therefore not only the intermolecular but also the coupling between the intermolecular and intramolecular motion has to play a role. Thus we conclude that in the regime of high multiphonon excitation at large collision energies both the inter- and intramolecular potentials have to be improved with respect to their anharmonic behavior.

The calculations, as well as the measurements, show only a marginal size dependence. This result is completely different from that observed for argon clusters, where the size dependence could be traced back to the collective breathing mode of a dense sphere.[4] Apparently the hydrogen-bonded network of the ammonia clusters, with their sixfold-coordinated bonds, prevents the cluster from collective excitation as in the case of the weakly bound van der Waals system, although the shape is spherical. This is similar to the result obtained for water clusters.[6]

The conclusion that we have drawn at the end of the experimental paper[9] by comparing the measured peaks at 14, 27, and 33 meV with the phonon spectrum of the crystal proved to be too simple. The peak at 33 meV, which is in the range of the librational mode of the solid, is definitely caused by the multiphonon excitation of the lowest-energy translational mode. The same is valid for the peak at 27 meV. Only the peak at 14 meV is close to the second band of the originally excited N···N···N bending mode (see Fig. 6, lowest panel). Interestingly, we missed in this experiment at the collision energy of 94.8 meV the main band of this motion at 7 meV which is clearly observed in the measurement at 50.5 meV displayed in Fig. 14.

This result nicely demonstrates the power and the problems of the helium atom scattering in revealing the vibrational frequency spectrum without performing calculations. The angular dependence gives us an interesting tool to distinguish between single and multiphonon excitations. But we have to make sure that also the collision energy is low enough to let us observe these features. Otherwise, the measured energy loss spectra are completely dominated by multiphonon processes that totally mask the original frequency curve.

ACKNOWLEDGMENTS

This work was supported by the Deutsche Forschungsgemeinschaft and the Alexander-von-Humboldt-Stiftung in the ''Forschungskooperation Europa.'' The authors thank Dr. R. Krohne for measuring the data of Fig. 2.

[1] See, for instance, the complete issue Chem. Rev. **100**, 3861 (2000).
[2] K. Liu, J. D. Cruzan, and R. J. Saykally, Science **271**, 929 (1996).
[3] U. Buck and R. Krohne, Phys. Rev. Lett. **73**, 947 (1994).
[4] U. Buck, R. Krohne, and P. Lohbrandt, J. Chem. Phys. **106**, 3205 (1997).
[5] T. Schröder, R. Schinke, U. Buck, and R. Krohne, J. Chem. Phys. **106**, 9067 (1997).
[6] J. Brudermann, P. Lohbrandt, U. Buck, and V. Buch, J. Chem. Phys. **112**, 11038 (2000).
[7] J. Brudermann, P. Lohbrandt, U. Buck, and V. Buch, Phys. Rev. Lett. **80**, 2821 (1998).
[8] J. Brudermann, U. Buck, E. Fredj, R. B. Gerber, and M. A. Ratner, J. Chem. Phys. **111**, 10069 (1999).
[9] U. Buck, R. Krohne, and S. Schütte, J. Chem. Phys. **106**, 109 (1997).
[10] C. Bobbert, S. Schütte, C. Steinbach, and U. Buck, Eur. Phys. J. D **19**, 183 (2002).
[11] T. Beu and U. Buck, J. Chem. Phys. **114**, 7848 (2001).
[12] R. Krohne, Ph.D. thesis, University of Göttingen, 1993; Max-Plack-Institut für Strömungsforschung, Göttingen, Report No. 18, 1993.
[13] U. Buck, F. Huisken, J. Schleusener, and J. Schaefer, J. Chem. Phys. **72**, 1512 (1980).
[14] C. Steinbach and U. Buck (unpublished results).
[15] S. Schütte and U. Buck, Appl. Phys. A: Mater. Sci. Process. **69**, S209 (1999).
[16] U. Buck, in *Atomic and Molecular Beam Methods*, edited by G. Scoles (Oxford University Press, New York, 1988), Chap. 21, p. 525.
[17] H. Meyer, U. Buck, R. Schinke, and G. H. F. Diercksen, J. Chem. Phys. **84**, 4976 (1986).
[18] Z. Bačić, U. Buck, H. Meyer, and R. Schinke, Chem. Phys. Lett. **125**, 47 (1986).
[19] D. C. Rapaport, *The Art of Molecular Dynamics Simulation* (Cambridge University Press, Cambridge, England, 1995).
[20] W. H. Press, S. A. Teukolsky, W. T. Vetterling, and B. P. Flannery, *Numerical Recipes in C: The Art of Scientific Computing*, 2nd ed. (Cambridge University Press, Cambridge, England, 1992).
[21] M. Diraison, G. J. Martyna, and M. E. Tuckerman, J. Chem. Phys. **111**, 1096 (1999).
[22] R. W. Impey and M. L. Klein, Chem. Phys. Lett. **104**, 579 (1984).
[23] G. Herzberg, *Molecular Spectra and Molecular Structure, Infrared and Raman Spectra of Polyatomic Molecules* (Van Nostrand Reinhold, New York, 1945).
[24] J. Huang and L. S. Bartell, J. Phys. Chem. **98**, 4543 (1994).
[25] J. W. Reed and P. M. Harris, J. Chem. Phys. **35**, 1730 (1961).
[26] O. S. Binbrek and A. Anderson, Chem. Phys. Lett. **15**, 421 (1972).
[27] P. S. Goyal, B. A. Dasannacharya, C. L. Thaper, and P. K. Iyengar, Phys. Status Solidi B **50**, 701 (1972).
[28] R. G. Della Valle, P. F. Fracassi, R. Righini, and S. Califano, Chem. Phys. **44**, 189 (1979).
[29] W. Y. Zeng and A. Anderson, Phys. Status Solidi B **162**, 111 (1990).
[30] P. de Pujo, J.-M. Mestdagh, J.-P. Visticot, J. Cuvellier, P. Meynadier, O. Sublemontier, A. Lallement, and J. Berlande, Z. Phys. D: At., Mol. Clusters **25**, 357 (1993).
[31] U. Buck, Comments At. Mol. Phys. **17**, 143 (1986).